

Final-state effects in the 3*d* photoelectron spectrum of Fe₃O₄ and comparison with Fe_xO

S. F. Alvarado, M. Erbudak, and P. Munz

Laboratorium für Festkörperphysik, Eidgenössische Technische Hochschule, 8093 Zürich, Switzerland

(Received 12 April 1976)

Photoelectron-spin-polarization measurements with photon energies up to 11 eV on Fe₃O₄ and energy distribution curves in the photon energy range $5 < h\nu < 90$ eV on magnetite (Fe₃O₄) and wustite (FeO) are interpreted in terms of the atomic theory of the single-ion-in-a-crystal-field model. The combination of the two different experiments yields the shapes and positions of the filled oxygen 2*p* bands and the 3*d*^{*n*-1} final states of Fe ions with a reliability previously not attained. The 3*d*^{*n*-1}-multiplet structure of Fe₃O₄ can be explained with the following set of parameters: $10Dq = 1.75$ eV and the Racah parameter $B = 645$ cm⁻¹ for Fe³⁺ left behind in *B* lattice sites; $10Dq = 1.55$ eV for Fe⁴⁺ in *A* sites. The difference in threshold for photoionization of Fe²⁺ and Fe³⁺ in *B* sites is 1.0 eV. The oxygen 2*p* emission is found to be centered at 7.3 eV below the Fermi level with a full width of 3 eV at half-maximum. The 3*d*-multiplet structure of Fe_xO can be explained with $10Dq = 1.7 \pm 0.1$ eV and $B = 800$ cm⁻¹.

INTRODUCTION

The electronic excitations from the 3*d* states of transition-metal (TM) ions in solids have been subject to constant investigations theoretically and experimentally.¹⁻⁵ The most interesting features in the electronic structure are observed in the region about 10 eV below the Fermi level, where the unfilled 3*d* states of the TM ion and the filled 2*p* oxygen bands are located. Some authors have proposed one-electron energy levels to describe the 3*d* photoelectronic excitations in magnetite.^{6,7} However, recently it was shown that a description in terms of band states cannot account for the observed optical excitations of certain TM oxides^{3,4,8}; they could only be explained and understood by methods of atomic physics. In a previous work² this new aspect was not considered and the data were interpreted by means of the simple band model.⁶ According to the model of a single ion in a crystal field (SICF), the photoelectronic excitations depend on the energy of the 3*d*^{*n*-1}-derived state of the metal ion left behind. There were also attempts to determine the energy separation of the localized 3*d* levels as well as the spectral features and level widths of the overlapping 3*d* states and oxygen 2*p* bands in simple TM.⁴ Yet magnetite is more complicated because it has two lattice sites and the Fe ion exists in two valencies. Energy distribution curves alone can never disentangle the different contributions. It is also different from the simple ionic TM oxides in that it exhibits a metal-insulator transition at 119°K.

Here we compare photoelectron-spin-polarization (ESP), and ultraviolet and far-ultraviolet photoemission-spectroscopy (UPS and FUPS) results on magnetite with the aim of showing that the SICF model correctly describes and explains the electronic excitation spectra of the Fe ions and that the latter indeed is representative for the ion-

ized state but not for the initial band density of states. The ESP results correctly locate the position of the unpolarized oxygen 2*p* emission and distinguish it from the 3*d* state emission. Further, we compare these results with those obtained from FeO, wustite, by FUPS with the purpose of supporting the earlier report⁴ and developing a deeper insight into the SICF model. This latter goal has been achieved by comparing the results with numerical calculations on the SICF model.

Fe forms various oxides. Fe_xO ($x = 0.90 - 0.95$) is an NaCl-type crystal and it is an antiferromagnet with a Néel temperature of 200°K. Fe₃O₄, on the other hand, is a ferrimagnet with a Néel temperature of 858°K, and crystallizes in the inverse cubic spinel structure, where the magnetic moments of the Fe³⁺ ions on *A* sites (tetrahedral) are aligned antiparallel to the moments of the remaining Fe³⁺ and Fe²⁺ ions occupying *B* sites (octahedral).

EXPERIMENT

The photoelectron-spin-polarization measurements were performed at photoenergies up to 11.2 eV. The spin polarization $P(h\nu)$ of the photoelectrons was measured by Mott scattering. $P(h\nu) = (n_{\uparrow} - n_{\downarrow}) / (n_{\uparrow} + n_{\downarrow})$ where n_{\uparrow} (n_{\downarrow}) is the yield of up-spin (down-spin) photoelectrons obtained with light of energy $h\nu$. The ESP measures thus the normalized difference between *A*- and *B*-site 3*d* emission in contrast to the energy distribution curve (EDC), which is a measure of the sum of all contributions.

The FUPS spectra were taken using synchrotron radiation obtained from the Cambridge Electron Accelerator in the range $5 \leq h\nu \leq 90$ eV, where electron energies were determined using a commercially available double-pass cylindrical mirror analyzer with a resolution of 0.20 eV. Since no

charging effects were observed on either material, the Fermi level was determined from an EDC on a gold foil freshly evaporated *in situ* on the cleaved crystal face.

The UPS measurements were performed in the energy range $7.85 \leq h\nu \leq 9.7$ eV. Energy distribution curves were measured with the retarding-field method with an energy resolution of 0.10 eV for all electrons emitted in half-space as well as for electrons emitted preferably within a limited solid angle. This latter delivered essentially the same structure in the EDC but showed better resolution, because smearing effects caused by the imperfection of the cleavage plane appear to have less influence.

All ESP, FUPS, and UPS measurements were made in ultrahigh vacuum ($p \sim 10^{-10}$ /Torr), with surfaces obtained by cleaving single crystals of Fe_xO and natural single crystals of Fe_3O_4 *in situ*. Most of the surfaces obtained after cleaving were irregular. A microprobe analysis on the magnetite crystals revealed on overall impurity concentration of less than 0.5 at.% for the important metallic impurities. For more-detailed information on the ESP, FUPS, and UPS measurements see Refs. 2, 9, and 10.

RESULTS

Figure 1 shows EDC's measured at $h\nu = 20$ and 30 eV on Fe_3O_4 , where the electron energies are plotted with respect to the Fermi level. The emission of inelastically scattered secondary electrons is subtracted from the EDC's to obtain the combined emission from overlapping *p*-band and *d*-state emissions. From results of ESP we know that the contribution of unpolarized oxygen electrons to the spectra at $E \approx 6$ eV is about 25% of the total number of electrons from *d* levels. This observation combined with the method reported earlier,⁴ which makes use of the energy dependence of 3*d* relative to 2*p* emission, was used to determine the spectrum from oxygen *p* bands (dashed lines). We observe that the oxygen 2*p* bands are about 3-eV full width at half-maximum, with the threshold at 4.7 eV and the peak at $E = 7.3$ eV. The structure near $E = 11$ eV has earlier been interpreted as a multielectron satellite⁴ but it is not relevant for the interpretation of the *d*-multiplet structure. The heavy curve is obtained when the inelastic secondaries and the oxygen emission are subtracted from the EDC's. Comparison of the two spectra in Fig. 1 reveals that the overall features of both *d*-state emissions at $h\nu = 20$ and 30 eV are the same and their emission intensity increases with photon energy as one goes from 20 to 30 eV with respect to oxygen 2*p* emission. Figure

2 shows angle-selective EDC's of Fe_3O_4 for the photon energy range $7.85 \leq h \leq 9.7$ eV. These curves show more structure than the EDC's at higher energies, and the peak position is independent of $h\nu$.

Preliminary SICF-model calculations of the magnetite ESP spectrum indicated, besides the positive polarization maximum observed at $h\nu \approx 7$ eV, the existence of a submaximum centered at $h\nu \approx 8.5$ eV. Since this submaximum was not well resolved in previously reported results,² more data were collected concentrating on the photon energy region between 7 and 10 eV. The existence of the predicted structure emerged clearly, as shown in results illustrated in Fig. 3. Analysis of all the available ESP spectra on Fe_3O_4 shows also that the spin polarization decreases below the saturation value of 25% at photon energies greater than about 9.5 eV, indicating that the onset of emission of unpolarized oxygen 2*p* electrons occurs at smaller photon energies than previously assumed.^{1,2}

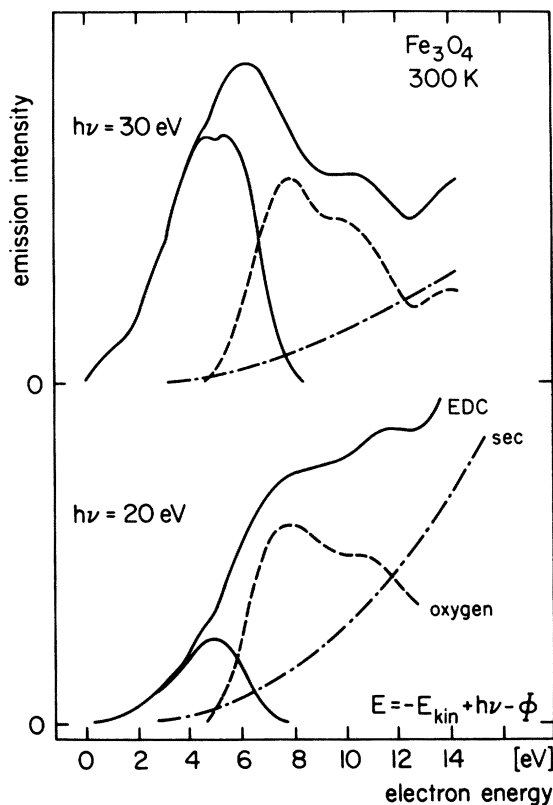


FIG. 1. Energy distribution curves (EDC's) with synchrotron radiation at $h\nu = 20$ and 30 eV. The Fermi energy $E_F = 0$, Φ is the work function, and E_{kin} is the kinetic energy of the photoelectrons. Inelastic secondaries dash-dot line and oxygen 2*p* emission (dashed line) are subtracted to obtain the 3*d* spectrum (solid line).

DISCUSSION

These spectra (Figs. 1–3) can be interpreted in terms of atomiclike excitations where one observes the multiplet structure of $3d^5$ final states of Fe^{2+} ions and $3d^4$ final states of Fe^{3+} ions rather than initial bandlike d density of states. Application of methods of atomic physics to explain phenomena in solid-state physics is described by Sugano *et al.*⁵ The method of fractional parentage yields the relative line intensities of the atomiclike localized final-state d -electron configurations. The energy position of the multiplets depends on the energy of the initial state determining the center of gravity of the whole set of multiplets. The splitting depends on the crystal field $10Dq$ and Racah (B) parameters and on the relaxation effects during the photoemission process. $10Dq$ and B were determined by fitting the theory⁵ to ESP, UPS, and FUPS data. The relative line intensities are commonly assumed to be proportional to $(2s+1)C_{(f)}^2$, where s is the spin and $C_{(f)}$ is the fractional-parentage coefficient of the final state. One has to take special care in incorporating the spin multiplicity $2s+1$; in the past it was not clear when to

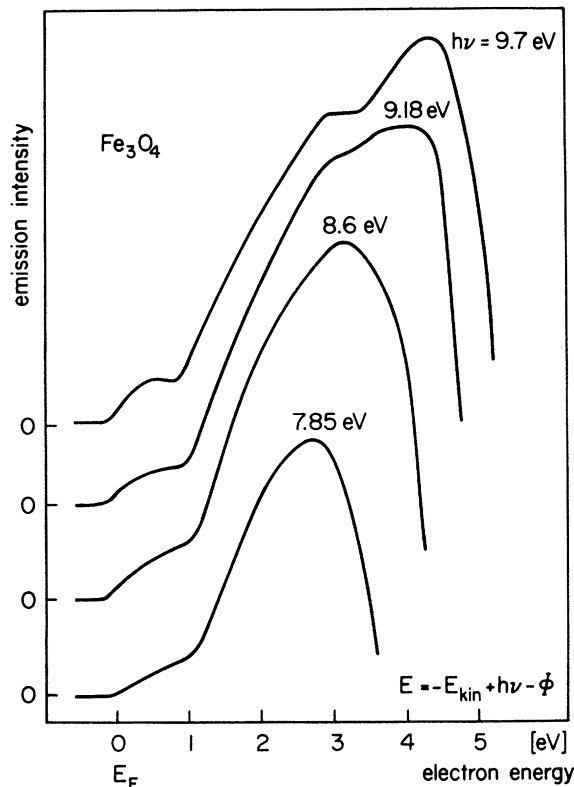


FIG. 2. Energy distribution curves at various photon energies (UPS). The intensity of photoemitted electrons is in arbitrary units.

apply it and when not.^{4,6,11} The multiplication with $2s+1$ is only allowed in cases of magnetic disorder with spin degeneracy. However, in the case of a magnetic order defining a z axis for the spins in cases of antiferromagnetic, ferrimagnetic, and ferromagnetic materials at temperatures below the Néel or Curie temperatures the spin degeneracy is removed owing to alignment of magnetic moments, and the spin multiplicity is not incorporated. In the case of Fe_3O_4 , which has a Néel temperature of 858°K , this factor should not be taken into account, contrary to the case of FeO , which has its ordering temperature at 200°K . Following this argument one should omit the spin-multiplicity factor for room-temperature measurements of NiO , which has a Néel temperature of 647°K . This reasoning was omitted in an earlier report.³ The Fe^{4+} and Fe^{3+} ions left behind in A and B sites after photoemission of an electron generate three multiplet groups: The Fe^{4+} in B sites produce the 5E_g and 5T_g lines which in the case of

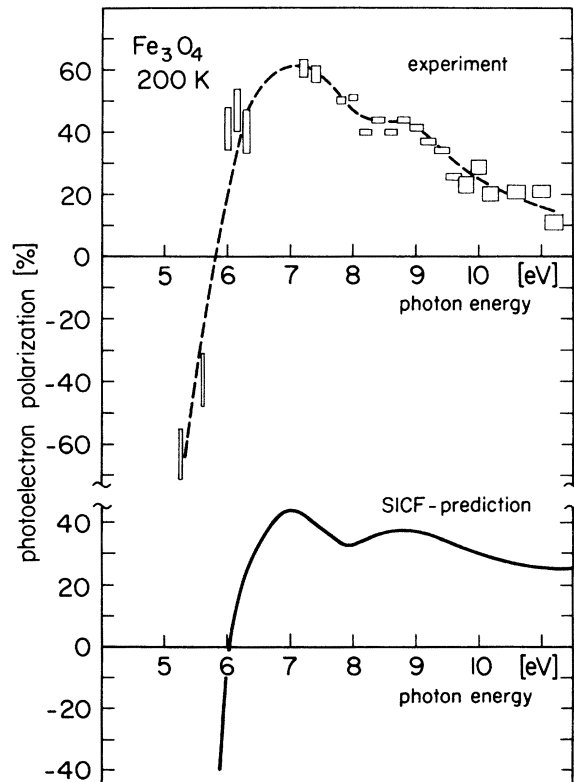


FIG. 3. Electron spin polarization (ESP) as a function of $h\nu$ and prediction of SICF model for Fe_3O_4 . Multiplets are as indicated in Fig. 4, but with a linewidth $\Delta m = 0.55$ eV. Photothreshold $\xi = 3.90 \pm 0.3$ eV. The photon energy at which the ESP decreases below the saturation value of 25% is different in each individual sample. The threshold for oxygen $2p$ emission is estimated to be at $h\nu = 9.5 \pm 0.6$ eV.

Fe^{4+} in A sites appear inverted in order. The reason for this is that the signs of the ligand field splitting in A and B sites are opposite.¹² The relative intensity between the 5T and 5E lines is theoretically $\frac{3}{2}$. The Fe^{3+} ions in B sites generate two subgroups of lines whose relative energy separation depends on the exchange energy between up- and down-spin electrons. Furthermore a measurement of this energy separation allows one to determine the Racah parameter with the aid of the multiplet diagrams of Sugano *et al.*⁵ The first subgroup is formed by a single line, the ${}^6A_{1g}$, which corresponds to photoemission of the down-spin minority electron of the $3d^6$ shell. ${}^6A_{1g}$ appears at $E \approx 0.5$ eV in both Figs. 1 and 2, and in ESP as negative polarization near photothreshold. The second subgroup of lines is generated when a majority (up-spin) electron is photoemitted.

The calculation of the spectra was done using the following simple model: (a) The current i_μ of photoelectrons obtained when the Fe ion is left in the final state μ is $i_\mu = I_\mu \{1 - \exp[-(h\nu - E_\mu)/K]\}$ for $h\nu > E_\mu$, and $i_\mu = 0$ for $h\nu \leq E_\mu$, where E_μ is the photothreshold and I_μ is the intensity of the transitions. The effect of the surface barrier in the electron escape probability is accounted for by the constant K , which is of the order of 1–2 eV.¹⁴ (b) The saturation photoelectron intensity from a $3d^n$ shell in a lattice site (s) is $I_s^*(3d^n) = \sum_\mu I_\mu$, where the sum is over all allowed final states which correspond to the occupancy (n). This quantity has been taken to be proportional to the number (n) of electrons in that shell, i.e., the rate $I_B^*(3d^6)/I_B^*(3d^5) = \frac{6}{5}$ for emission from Fe^{2+} and Fe^{3+} ions in B sites and $I_A^*(3d^5)/I^*(3d^5) = 1$ for emission from Fe^{3+} ions in A and B sites. (c) For Fe_3O_4 the ideal ratio of $10Dq$ at B and A sites is $\Delta_B/\Delta_A \sim 1.1$.¹² Therefore only one crystal field parameter is required to fit the data. (d) To account for the multiplet broadening due to lifetime effects and smearing of the photothreshold due to irregular sample surfaces, simple Gaussian line shapes¹⁵ of linewidth Δm have been chosen. EDC's are calculated by superimposing the $3d^{n-1}$ multiplets. Figure 4 shows the results of the calculation, which compares favorably with both the FUPS and UPS results in that most of the structure is reproduced.

The peak at 4.7 eV for the EDC taken at $h\nu = 20$ eV is relatively larger than the one shown in the calculated curve; this indicates that the shape of the oxygen $2p$ contribution should be steeper at its photothreshold than the one given in Fig. 1. The difference between the experimental and theoretical EDC's can be due to the following: (i) Because of reduced escape depth the FUPS EDC's might be smeared to a larger extent owing to perturbations at the surface. (ii) The fact that the EDC's

at $7.85 \leq h\nu \leq 9.7$ eV are measured only for electrons emitted within a restricted solid angle is not considered in the model calculation. (iii) The bad cleaving properties of magnetite may result in some smearing of the curves. It is expected that this smearing diminishes with increasing electron kinetic energy, which is observed in the EDC's of Figs. 1 and 2 for the shoulder at $E \sim 0.5$ eV.

The ESP spectrum is calculated with $n_\uparrow = \sum_\mu i_\mu(\uparrow)$, where the sum is over all the multiplets which contribute with up-spin electrons; n_\downarrow is calculated

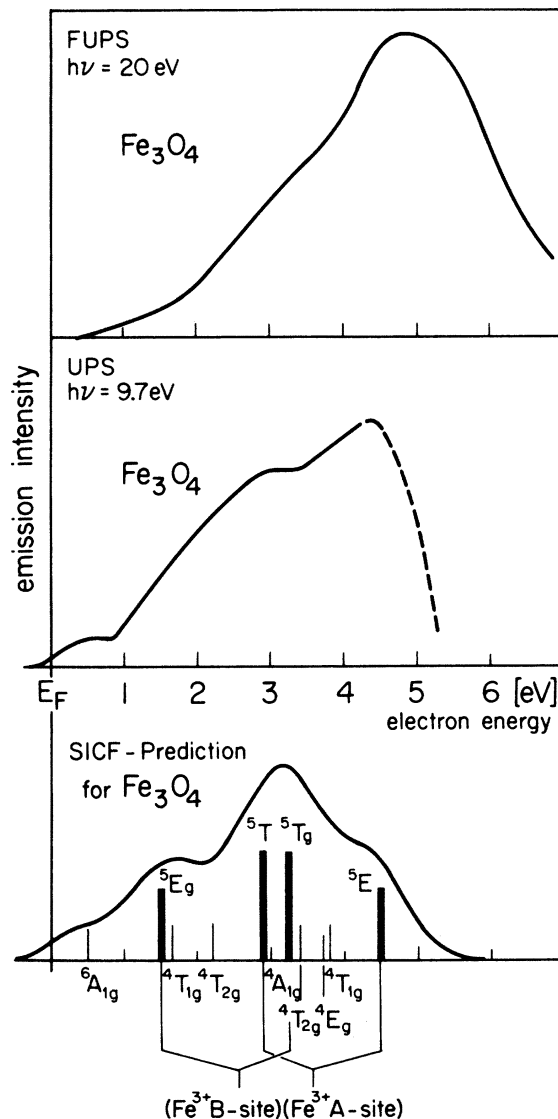


FIG. 4. $3d$ emission as observed with synchrotron radiation (FUPS), with ultraviolet light (UPS), and as calculated with the single-ion-in-a-crystal-field (SICF) model with the parameters given in the text; the linewidth was assumed to be 1.25 eV for FUPS and 1.0 eV for UPS, but only the last case is shown.

correspondingly.

The best fitting to ESP and EDC data is obtained for the following set of multiplet lines (energies in eV with respect to ${}^6A_{1g}$): for Fe^{3+} in *B* sites (all spin up except ${}^6A_{1g}$, which yields spin-down electrons): ${}^6A_{1g}$ [0], ${}^4T_{1g}$ [1.15], ${}^4T_{2g}$ [1.66], ${}^4A_{1g}$ [2.66], ${}^4T_{2g}$ [2.91], 4E_g [3.23], ${}^4T_{1g}$ [3.3]; those from Fe^{4+} in *B* sites (all spin up): 5E_g [1.01], ${}^5T_{2g}$ [2.75], and from Fe^{4+} in *A* sites (all spin down): 5T_2 [2.45], 5E [4.0].

The parameters are as follows: For Fe in *B* lattice sites, $10Dq = 1.75$ eV (Fe^{3+} and Fe^{4+} ions), $B = 645$ cm^{-1} (Fe^{3+} ion), $Dq/B = 2.19$ (high spin). The photoemission threshold for Fe^{3+} is 1 eV below ${}^6A_{1g}$. In *A* sites we have $10Dq = 1.55$ eV and photoemission threshold for Fe^{3+} 2.45 eV below ${}^6A_{1g}$. The parameters given above are practically independent of the linewidth and of the escape constant *K*. The EDC shown in Fig. 4 has been calculated with the above given set of multiplet lines and assuming a linewidth of 1.25 eV for FUPS and 1 eV for UPS.

Figure 3 illustrates the spin polarization calculated with the same multiplet structure but with a linewidth of 0.55 eV, escape constant $K = 1.5$ eV.¹⁴ The agreement between experiment and theory is even better for the ESP.

There is a deviation from the calculated curve in that the peak at $h\nu \sim 7$ eV is found experimentally to have a polarization $\sim 55\%$ whereas the model predicts 42%. The reason for this is that the real multiplet intensities might be slightly different from the values calculated with the coefficients of fractional parentage. For instance, with a 25% reduction of the ${}^6A_{1g}$ line the SICF calculation fits the experimental data almost perfectly. This intensity reduction could be justified by the EDC's in Fig. 2, which show that this line is quite sensitive to changing photon energies. But for the sake of clarity only the calculations performed with the ideal intensities are reported. The linewidth determined from the ESP fitting is substantially smaller than the values obtained from the EDC's. This can be explained by considering that the ESP is the normalized difference between up- and down-spin electron emission, and is therefore less sensitive than energy analysis to broadening of the lines caused by surface perturbations and apparatus resolution. Thus ESP seems to give a more reliable measure of the inherent linewidth.

In this context we would like to draw a parallel to the FUPS results on Fe_xO . Figure 5 shows EDC's taken at $h\nu = 20, 30,$ and 87 eV; all energies are plotted with respect to the Fermi level. In the lowest curve we have subtracted from the EDC the inelastically scattered secondaries and the contribution from the oxygen $2p$ bands to get

the *d*-state emission (solid line). The high-energy end of the oxygen bands was taken as similar to that from Fe_3O_4 . Oxygen bands and secondaries are not shown at spectra for $h\nu = 30$ and 87 eV for clarity. We observe, as in the case of Fe_3O_4 , that the total relative emission intensity from *d* states increases at higher photon energies, whereas the shape of the spectrum remains unchanged within experimental accuracy.

The best fitting of the EDC data on Fe_xO is obtained for the following set of multiplet lines (energies in eV with respect to ${}^6A_{1g}$): ${}^6A_{1g}$ [0], ${}^4T_{1g}$ [1.8], ${}^4T_{2g}$ [2.44], ${}^4A_{1g}$ [3.31], ${}^4T_{2g}$ [3.62], 4E_g [4.03], ${}^4T_{1g}$ [4.1]. The Racah parameter is $B = 800$ cm^{-1} and $10Dq = 1.7 \pm 0.1$ eV. The spectrum is calculated with a linewidth $\Delta m = 1.5$ eV and is illustrated in Fig. 6. The vertical lines represent

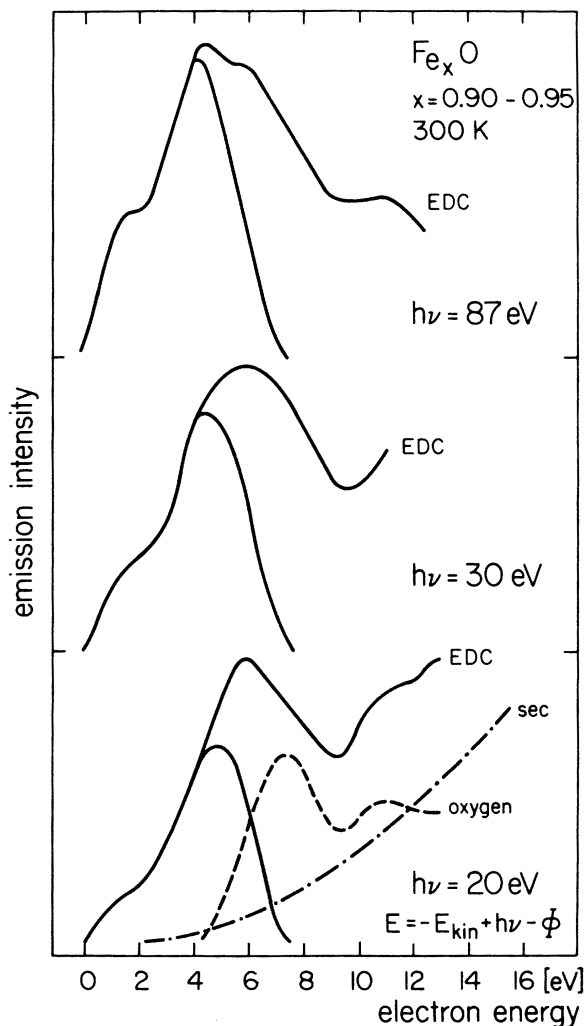


FIG. 5. EDC's at $h\nu = 20, 30,$ and 87 eV on wustite (Fe_xO , $0.90 < x < 0.95$).

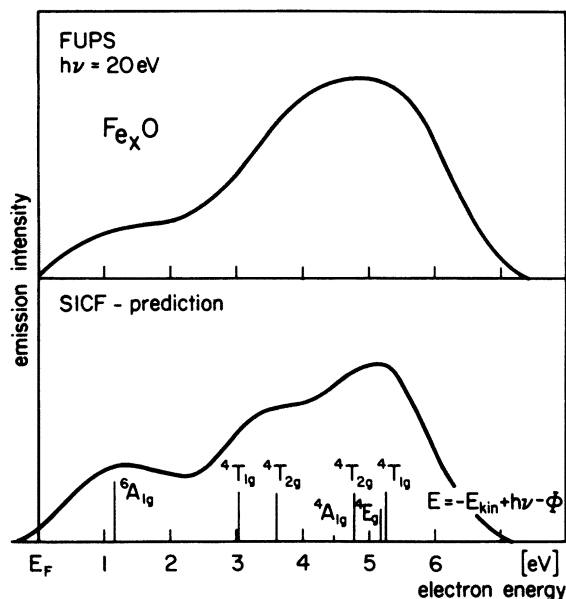


FIG. 6. Comparison between FUPS and the SICF model for Fe_xO . $10Dq = 1.7 \pm 0.1$ eV, Racah parameter $B = 800$ cm^{-1} , and linewidth of 1.5 ± 0.1 eV give the best fit.

the theoretical transition intensities. In the calculation we have multiplied the line intensities by $2s + 1$ since the experiments were performed well above the magnetic ordering temperature of FeO . This interpretation is in agreement with previously published work^{3,4} except for the position and the shape of the oxygen $2p$ bands. This latter discrepancy causes a distortion of the d -state emission in the former report.

It is interesting to compare the magnitude of the

Racah parameters for Fe^{2+} in Fe_3O_4 and Fe_xO with the free-atom value of $B = 917$ cm^{-1} .⁶ The reduced value of the B parameter in the oxides is due to the nephelauxetic effect,¹³ amounts to 30 and 13% in Fe_3O_4 and Fe_xO , respectively, and is possibly explained by a larger $2p$ - $3d$ hybridization in magnetite.

In conclusion, the SICF model correctly predicts the photoelectron excitation spectrum of magnetite observed in two complementary experiments, one of which is a measure of the sum of all the contributions (EDC's) and the other a measure of the normalized difference of up- and down-spin emission (ESP). The difficult question about the onset of the $2p$ oxygen emission is answered with higher reliability. With the aid of the results from magnetite we can also obtain more-refined insight into the electronic excitations of wustite. The numerical calculations based on the SICF model correctly predict the gross features of the observed spectra, which show that the state of the hole left behind plays a vital role for the interpretation of photoemission experiments on these oxides. There are also deviations of the spectra from the SICF prediction, which wait for a more-refined theoretical analysis.

ACKNOWLEDGMENTS

The authors are indebted to H. C. Siegman for helpful discussions and to P. Bagus for kindly providing calculations of fractional-parentage coefficients (unpublished). One of us (M. E.) wishes to thank D. E. Eastman and J. L. Freeouf for their generous contribution in obtaining the FUPS data. Part of this work was supported by the Schweizerischer Nationalfonds.

¹S. G. Bishop and P. C. Kemeny, *Solid State Commun.* **15**, 1877 (1974).

²S. F. Alvarado, W. Eib, F. Meier, D. T. Pierce, K. Sattler, H. C. Siegmann, and J. P. Remeika, *Phys. Rev. Lett.* **34**, 319 (1975).

³G. K. Wertheim, H. J. Guggenheim, and S. Hüfner, *Phys. Rev. Lett.* **30**, 1050 (1973).

⁴D. E. Eastman and J. L. Freeouf, *Phys. Rev. Lett.* **34**, 395 (1975).

⁵S. Sugano, Y. Tanabe, and M. Kamimura, *Multiplets of Transition Metal Ions in Crystals* (Academic, New York, 1970).

⁶D. L. Camphansen, J. M. D. Coey, and B. K. Chakraverty, *Phys. Rev. Lett.* **29**, 657 (1972).

⁷I. Balberg and S. I. Paknove, *Phys. Rev. Lett.* **27**, 1371 (1971).

⁸S. F. Alvarado, W. Eib, H. C. Siegmann, and J. P.

Remeika, *Phys. Rev. Lett.* **35**, 860 (1975).

⁹D. E. Eastman, W. D. Grobman, J. L. Freeouf, and M. Erbudak, *Phys. Rev. B* **9**, 3474 (1974).

¹⁰P. Cotti and P. Munz, *Phys. Kondens. Mater.* **17**, 307 (1974); P. Munz, *Helv. Phys. Acta* **49** (1976).

¹¹G. K. Wertheim and S. Hüfner, *Phys. Rev. Lett.* **28**, 1028 (1972).

¹²M. T. Hutchins, in *Solid State Physics*, edited by F. Seitz and D. Turnbull (Academic, New York, 1964), Vol. 16, p. 237.

¹³C. K. Jorgensen, *Modern Aspects of Ligand Field Theory* (North-Holland, Amsterdam, 1971).

¹⁴D. E. Eastman, *Techniques of Metals Research* (Interscience, New York, 1972), Vol. VI.

¹⁵Rigorously, the lifetime effects impart a Lorentzian broadening to the lines; however, Gaussian shapes were chosen for mathematical simplicity.